ELSEVIER

Catalysis Today 31 (1996) 79–91

CATALYSIS TODAY

Development of temperature-independent quantitative structure/reactivity relationships for metal- and acid-catalyzed reactions

S.C. Korre [1], M.T. Klein *

Center for Catalytic Science and Technology, Department of Chemical Engineering, University of Delaware, Newark, DE 19716, USA

Abstract

Hydrocracking of a mixture of naphthalene and phenanthrene in the temperature interval 300–370°C offered information on the temperature dependence of rate, equilibrium and adsorption constants. The number of parameters needed to describe phenanthrene and naphthalene hydrocracking kinetics was then reduced by the development of temperature-independent quantitative structure/reactivity relationships (QSRRs) for the activation and reaction enthalpies and entropies. Activation energies for isomerization and ring opening reactions were correlated with the heat of formation of the intermediate carbocation. Activation energies for hydrogenation were correlated with the standard reaction enthalpy. The principle of compensation was successfully used to relate entropic quantities to enthalpic quantities. The existence of QSRRs allowed the kinetics of naphthalene and phenanthrene hydrocracking to be represented very satisfactorily, over a wide temperature range, in terms of just 17 QSRR parameters. These 17 parameters summarized the chemical information in 576 rate, equilibrium, and adsorption constants. Thus, the QSRR approach reduced the number of modeling parameters by about 97%.

Keywords: Temperature-independent quantitative structure/reactivity relationships; Metal-catalyzed reactions; Acid-catalyzed reactions

1. Introduction

The increased interest in the molecular modeling of hydrocarbon conversion processes is motivated by the need to predict both the performance and environmental properties of the products. A molecular description of the hydrocarbon mixture is the logical starting point for these predictions, which has motivated considerable interest in the development of molecular reaction models.

The construction of such models is complicated by the enormous need for rate, adsorption and equilibrium parameters. This staggering need can be reduced considerably when the homologous patterns of both compound types and their reactions in these mixtures is recognized. This has motivated the development of a lumping approach that organizes the kinetics information in potentially thousands of rate, adsorption, and equilibrium constants into the parameters of a handful (O(10)) of quantitative structure reactivity relationships (QSRR) using

* Corresponding author.

[1] Present address: Exxon Engineering, P.O. Box 101, Florham Park, NJ 07932, USA.

PII S0920-5861(96)00022-3

the formalism of linear free energy relationships, first developed by Hammett [1].

The relevance of linear free energy relationships (LFER) in reactions heterogeneously catalyzed by acids was established by a series of articles by Mochida and co-workers. They correlated rate constants for dealkylation of alkylbenzenes with the enthalpy change for hydride abstraction from the related paraffin as a reactivity index [2]. The LFER parameters for a set of acid-catalyzed reactions depended only on the type of catalyst [3] and the kind of reaction. Similar correlations were found during isomerization of dialkyl benzenes [4]. A review of the LFER theory on acid-catalyzed reactions is available [5].

The application of these ideas to hydrocracking of polynuclear aromatics is more recent. For example, Landau et al. [6] verified the applicability of the LFERs to dealkylations of butyl tetralins. Neurock and Klein [7,8] revisited the experimental data of Mochida et al. to show that the standard enthalpy of reaction of the controlling elementary step could be used as a reactivity index instead of the enthalpy of hydride abstraction from the paraffin. This was valid for both dealkylations and isomerizations, and resulted in unifying several correlations using a single reactivity index. These investigators also developed QSRRs for hydrogenations of polynuclear aromatics using electronic properties as reactivity indices (π-electron density). In addition to electronics reactivity indices, Korre et al. [9] used the standard enthalpy of reaction to correlate rate and equilibrium constants in the hydrogenation of polynuclear aromatics.

All of the foregoing work was limited to a set of "isothermal correlations," i.e. one correlation was developed for each temperature. Mochida and Yoneda [10] have hinted at the extension of their earlier work with LFERs for activation energies. Clearly, a more universal, temperature-independent correlation would be desirable. The present work aimed to exploit this concept and explore (1) the applicability of QSRRs to the acid-center transformations during hydrocracking, and (2) the dependence of QSRRs on temperature for both metal- and acid-catalyzed reactions. The tangible result of such correlations would be the organization of energetic and entropic quantities for both overall reaction and activation for a wide range of hydrocracking reactions.

The literature establishes the need for such information on heavy oil hydrocracking. Available information on activation energies and pre-exponential factors is generally fragmented and catalyst-dependent. The effect of temperature on PNA reactions over zeolite-supported metal sulfide catalysts has not been explored in detail. The kinetics information for the metal function usually pertains to hydroprocessing catalysts, whereas most studies on the acid function have focused on FCC catalysts and conditions. Finally, most studies determine apparent activation energies based on pseudo-first order rate constants.

Reported PNA saturation activation energies over hydroprocessing catalysts are in the range of 7–12 kcal/gmol [11,12]. This range is valid over a wide temperature interval (190–315°C for the former study, 450–500°C for the latter). Apparent activation energies for acid center transformations (i.e. paraffin isomerization and cracking reactions) are substantially higher, of the order of 20–40 kcal/gmol. This is frequently related to the formation of energetically demanding carbocation intermediates.

The absence of consistent experimental information in the literature helped motivate the present study aimed at exploring the temperature dependence of hydrocracking reaction rate laws. To this end, separation of rate, equilibrium and adsorption parameters was necessary for the successful development of structure–reactivity correlations. The development of quantitative reaction networks and rate laws for naphthalene and phenanthrene hydrocracking at 350°C was described elsewhere [13]. In this paper, the reactions of a mixture of naphthalene and phenanthrene in the interval 300–370°C were used to evaluate Arrhenius and van't Hoff

Table 1
Conditions for the temperature effect experiments.
N = naphthalene; P = phenanthrene; x = fractional conversion

T (°C)	P_{chx} (atm)	$N_0/(N_0+P_0)$	Time (h)	x_N	x_P
300	74.9	0.582	4.00	0.894	0.867
310	81.7	0.588	3.00	0.872	0.911
320	95.3	0.584	3.33	0.948	0.964
330	102.1	0.577	3.00	0.951	0.977
340	112.3	0.582	3.25	0.950	0.982
350	122.5	0.580	1.83	0.889	0.933
365	136.1	0.584	2.25	0.943	0.973
370	149.8	0.575	2.25	0.916	0.977
Average		0.581		0.920	0.948
St. Dev. (%)		0.69		3.46	4.37

parameters for rate, equilibrium and adsorption constants. These were correlated with appropriate reactivity indices, resulting in a significant reduction in the number of parameters needed to describe hydrocracking kinetics in a wide temperature interval.

2. Experimental results

A 1-l batch autoclave equipped with reactant injection and sample procurement systems was used as described elsewhere [14,15]. The catalyst was 10 g of a process-treated Zeolyst hydrocracking catalyst (NiW/USY). Naphthalene and phenanthrene hydrocracking were studied over the temperature range of 300–370°C, at the 10°C intervals listed in Table 1. This range was selected taking into consideration both the relevant hydrocracking conditions in industrial practice as well as experimental limitations.

The reactant mixture consisted of 30 g of a 50 wt% mixture of naphthalene and phenanthrene, dissolved in 15 g of cyclohexane. Detailed composition analysis up to high conversions ensured a wide sampling of naphthalene/phenanthrene compositions with this starting composition. The effect of hydrocarbon and ammonia inhibition on naphthalene and phenanthrene hydrocracking is discussed extensively in a separate paper [13].

The reactant mixture was introduced in 400 g of cyclohexane as a solvent at the arbitrary $t = 0$ time with hydrogen back pressure. The solvent was in a supercritical state (one phase) at all conditions, and the hydrogen pressure was varied from 62 atm (300°C) to 70 atm (370°C) in order to ensure constant hydrogen concentration of 1.33 gmol/l during all experiments. Solvent reactions (cyclohexane isomerization to methyl cyclopentane, bimolecular disproportionation [15]) were severely suppressed in the presence of the polynuclear aromatics [13,15]. Phenanthrene and its hydrocracking products inhibited cyclohexane isomerization more than naphthalene and its hydrocracking products.

Naphthalene hydrocracking products included tetralin, *n*-butyl benzene, 1-, 2-, 3-, and 4-methyl indans, indan, *trans*-decalin, *cis*-decalin and decalin isomers, as well as smaller amounts of alkylbenzenes, alkylcyclohexanes, methyl naphthalenes, and methyl tetralins. Identified products from phenanthrene hydrocracking included dihydrophenanthrene, tetrahydrophenanthrene and isomers of molecular weight 182, *sym*- and *asym*-octahydrophenanthrenes and isomers of molecular weight 186, methyl-, ethyl- and butyl tetralins, tetralin, naphthalene, methyl indans, indan, butyl benzene and other alkyl benzenes. There was no evidence of dimethyl- or ethyl-biphenyls. All products were identified by co-injections and mass spectral information.

The reaction duration was adjusted in order to obtain final conversions higher than 90% from all experiments. The evolution of phenanthrene and naphthalene conversion with time for the conditions of Table 1 is presented in Fig. 1. Conversion rates for both reactants were accelerated with increasing temperature. The effect of temperature was more pronounced at temperatures lower than 350°C. At the temperatures of 350, 365, and 370°C the influence of thermodynamic equilibrium on PNA hydrogenations began to appear.

The observed products index, defined as the weight of identified products divided by reactant weight converted, for naphthalene and phenanthrene hydrocracking was essentially

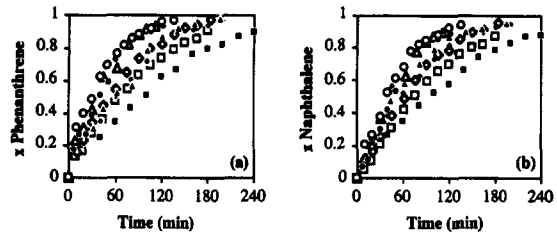

Fig. 1. Evolution of phenanthrene (a) and naphthalene (b) hydrocracking conversion with time as a function of reaction temperature. (■) 300°C; (□) 310°C; (♦) 320°C; (◇) 330°C; (▲) 340°C; (△) 350°C; (●) 365°C; (○) 370°C.

unity at all times at the lowest temperature of 300°C. It decreased, predictably, thereafter with increasing temperature, presumably due to the formation of light gases. Naphthalene/tetralin production from phenanthrene only occurred at high phenanthrene conversion ($x > 0.8$), and the amounts produced at 50% wt were too low to interfere with the analysis of naphthalene hydrocracking kinetics, which could be determined from the lower conversion data [13].

Naphthalene and phenanthrene hydrocracking product yields with respect to reactant conversion at the temperatures of Table 1 are presented in Fig. 2. Fig. 2a indicates that virtually all naphthalene was converted to tetralin at all temperatures, up to naphthalene conversion of approximately 0.6. At higher naphthalene conversions, the maximum in tetralin yield decreased with increasing temperature. This implies that tetralin consumption rates had a stronger temperature dependence than its formation rate from naphthalene hydrogenation. For irreversible reactions, a stronger temperature dependence is associated with a higher activation energy.

The effect of temperature on the yields of di- and tetra-hydrophenanthrene with respect to phenanthrene conversion is presented in Fig. 2b and Fig. 2c, respectively. The maximum yields for di- and tetra-hydrophenanthrene did not significantly diverge from 0.08 and 0.14, respectively, for all reaction temperatures. This indicates that their production and consumption reactions had a similar temperature dependence.

The variation of yields of *sym*-octahydrophenanthrene and *i*-tetrahydrophenanthrene with respect to reactant conversion are presented in Fig. 2d and Fig. 2e, respectively. The maximum yield in both cases shifted with increasing temperature, decreasing for *sym*-octahydrophenanthrene and increasing for *i*-tetrahydrophenanthrene. It therefore seems likely that the acid-catalyzed isomerizations consuming *sym*-octahydrophenanthrene had a stronger temperature dependence than the metal-catalyzed hydrogenations that produce it. This was also the case for *asym*-octahydrophenanthrene. On the contrary, the acid-catalyzed ring opening consuming *i*-tetrahydrophenanthrene had a weaker temperature dependence than the acid-catalyzed isomerizations that produce it.

The maximum yield of *i-sym*-octahydrophenanthrene slightly decreased with increasing temperature, as Fig. 2f attests. Ring opening products (*n*-butyl benzene, *n*-butyl

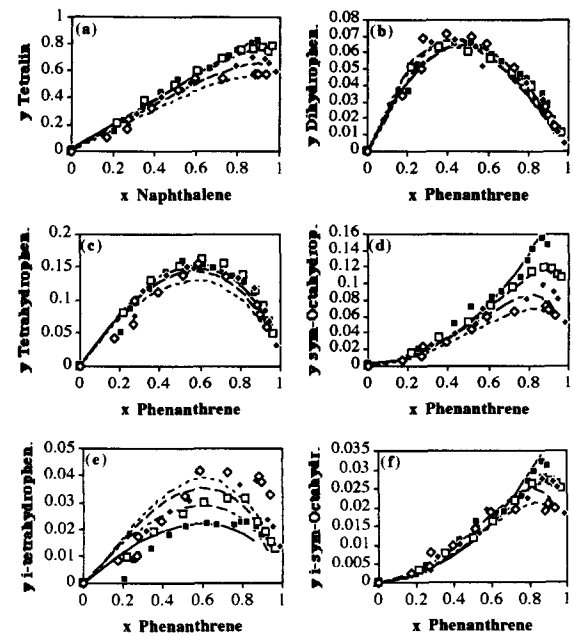

Fig. 2. Comparison between experimental and best-fit yields of phenanthrene and naphthalene hydrocracking products. (a) Tetralin; (b) dihydrophenanthrene; (c) tetrahydrophenanthrene; (d) *sym*-octahydrophenanthrene; (e) *i*-tetrahydrophenanthrene; (f) *i-sym*-octahydrophenanthrene. (■) 300°C; (□) 320°C; (♦) 340°C; (◇) 365°C.

naphthalene, 5- and 6-butyl tetralins, and 1- and 2-butyl tetralins) also exhibited lower yields with increasing temperature.

The development of the naphthalene and phenanthrene hydrocracking networks was discussed extensively in a separate publication [13]. The network is presented in Fig. 3. In summary, hydrogenation of aromatic rings on the metal sites (as in naphthalene, tetrahydrophenanthrene, terminal ring of phenanthrene) results in the creation of hydroaromatic structures (such as tetralin, octahydrophenanthrenes, tetrahydrophenanthrene). These, in turn, are subject to isomerization on the acid sites to methylindanes, methylcyclopenta-tetralins and naphthalenes. Ring opening to a butyl side chain was shown to proceed primarily through these isomerized structures [13,15]. Phenanthrene hydrogenation in the middle ring to dihydrophenanthrene was a dead end in the network: neither alkyl biphenyls nor increased toluene yields were observed, and hydrocracking of dihydrophenanthrene as the reactant showed phenanthrene as the only primary product [13,15].

The network of Fig. 3 allowed a first-pass estimate of the parameters of the dual-site

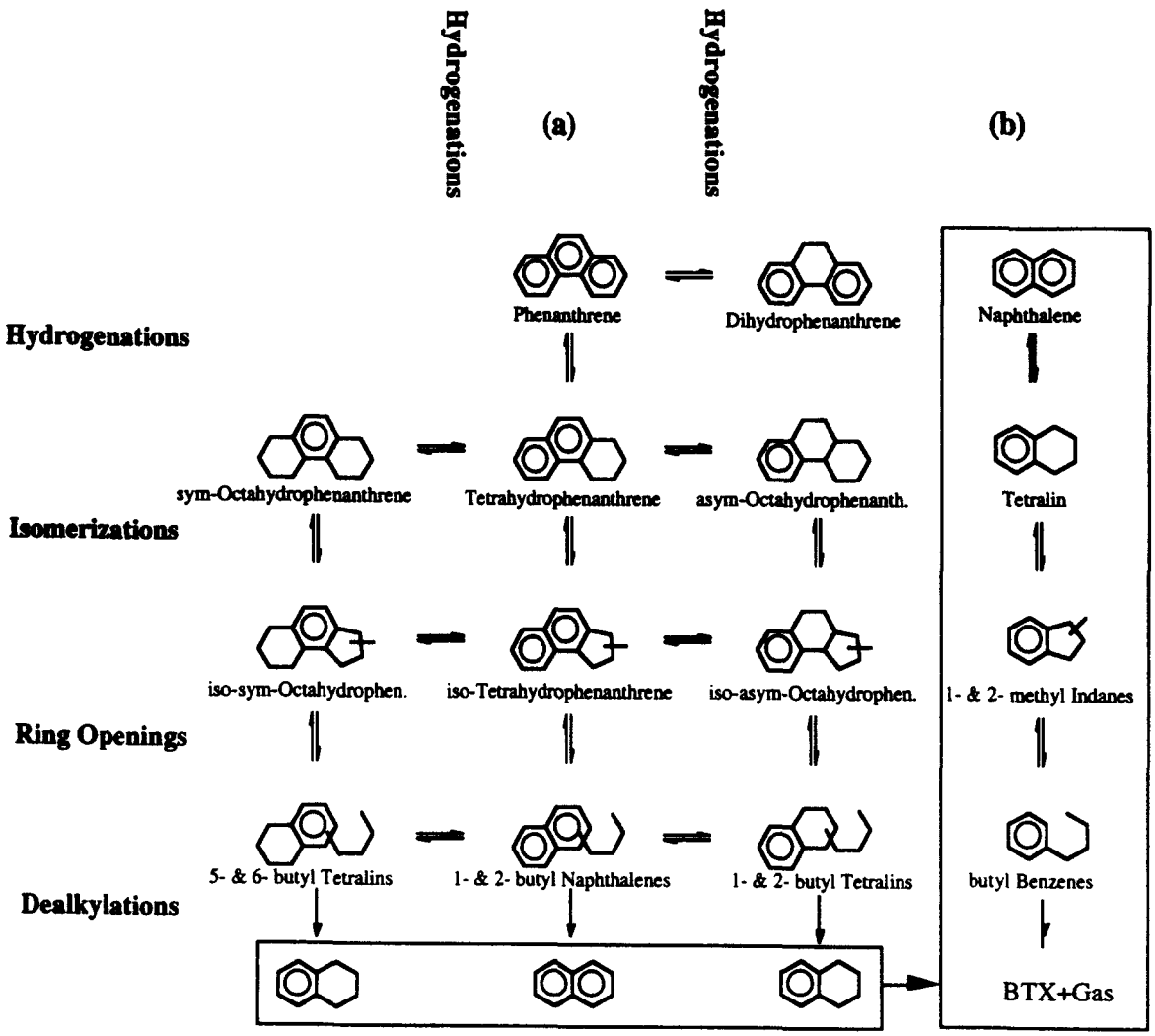

Fig. 3. Reaction families of hydrogenation, isomerization, ring opening and dealkylation in phenanthrene (a) and naphthalene (b) hydrocracking network.

LHHW (Langmuir–Hinshelwood–Hougen–Watson) rate expression of Eq. (1) [13,15].

$$-\frac{V_R}{W_{cat}}\frac{dC_i}{dt} = \frac{\sum_j k_{ij}(C_i - C_j/K_{ij})}{D_H} + \frac{\sum_l k_{il}(C_i - C_l/K_{il})}{D_A} \quad (1)$$

Eq. (1) is derived from the standard LHHW formalism (for example, see [16]). In Eq. (1), W_{cat} is the catalyst weight (10 g), V_R is the reactor volume (1 l), C_i, C_j, C_l are component concentrations (mol l^{-1}). k_{ij} and k_{il} are combined numerator rate parameters (l kg_{cat}^{-1} s^{-1}), and K_{ij}, K_{il} are the equilibrium ratios (mol_j/mol_i). It follows that the equilibrium ratio is equal to the equilibrium constant ($mol_j/mol_i/P_{H_2}^n$) multiplied by the hydrogen pressure (P_{H_2}) to the hydrogen stoichiometry (n). D_H and D_A were the adsorption groups for the metal (hydrogenation, $_H$) and zeolite (acid, $_A$) sites, respectively: $D_H = 1 + \sum_i K_i^H C_i$, $D_A = 1 + \sum_i K_i^A C_i$: K_i^H, K_i^A (l mol^{-1}) represented individual component adsorption constants on the metal and acid sites, respectively. Implicit is the assumption of surface reaction as the rate determining step. We found no statistical difference between models using one and two as the exponent of the adsorption group D_A, thus the simpler value of one was retained [9,13,15]. To the extent that the dual-site LHHW expression captures the rate, equilibrium, and adsorption phenomena in hydrocracking, the parameters thus estimated should be valid over a wide composition range, since competitive inhibition is directly accounted for in the LHHW formalism.

For each of the eight reaction temperatures, a total of 23 numerator rate parameters were regressed [k_{ij} in Eq. (1)], five for the naphthalene hydrocracking network of Fig. 3a, and 18 for the phenanthrene hydrocracking network of Fig. 3b. An equal number of equilibrium ratios [K_{ij} in Eq. (1)] were also regressed. Thus, a total of 368 numerator rate parameters and equilibrium ratios were required to represent the kinetics of naphthalene and phenanthrene hydrocracking in the temperature interval 300–370°C, summarizing approximately 1600 experimental concentration measurements. Parameter estimation results are represented as the curves in Fig. 2, and the overall agreement between experimental and calculated concentration profiles is very good. The sum-of-squares error on concentrations was less than 5×10^{-3} at all temperatures.

All reactions were generally enhanced with increasing temperature. Ring openings generally proceeded through larger rate constants than both isomerizations and hydrogenations. The exception was the tetrahydrophenanthrene sequence, where the isomerization rate constant was quite large. Isomerization proceeded with larger rate constants than hydrogenation for the tetrahydrophenanthrene and *sym*-octahydrophenanthrene sequence. Dealkylation rate constants for all butyl-substituted molecules were negligible at temperatures lower than 350°C. The cross-hydrogenation rate constants for the hydrogenation reactions of *i*-tetrahydrophenanthrene to *i-sym-* or *i-asym*-octahydrophenanthrene, and of *n*-butyl naphthalene to 5- and 6-butyltetralins or 1- and 2-butyl tetralins, were negligible at the highest temperatures, and became significant at the lowest temperatures only. At all temperatures, however, terminal ring hydrogenations proceeded with the largest rate parameters. In terms of structural ranking, rate parameters for transformations of tetralinic structures were lowest, while rate parameters for transformations of naphthalenic structures were highest.

The values of the equilibrium ratios for hydrogenations were much larger than unity at all temperatures, and decreased with increasing temperature, as expected for exothermic reactions. Equilibrium ratios for isomerizations were generally less than unity and increased with temperature, as expected for endothermic reac-

tions. Ring opening equilibrium ratios varied from 0.1 to 10, suggesting significant ring closure rates, and generally decreased with increasing temperature, consistent with exothermic reactions. Ring closure appeared more prompt for *n*-butyl naphthalene and *n*-butyl benzene and less so for 5- and 6-butyl tetralins and 1- and 2-butyl tetralins. Finally, dealkylation equilibrium ratios were much larger than unity at all temperatures, indicating virtually irreversible reactions.

3. Parameter reduction using QSRRS

The foregoing parameter estimation information shows that even the relatively simple 17-component networks of naphthalene and phenanthrene required 38 rate and equilibrium constants and 17 adsorption constants at each temperature. Extrapolation to the demands of a heavy oil suggests that a lumping strategy aimed at representing this information in terms of fewer parameters would be useful. To this end, it seemed cogent to attempt to organize the hydrocracking reactions into reaction families, which could in turn be characterized by quantitative structure–reactivity relationships.

Fig. 3 also illustrates the concept of reaction families in the naphthalene/phenanthrene network. Terminal-ring aromatics are subject to metal-catalyzed hydrogenation. The resulting cyclohexa-structures are undergoing acid-catalyzed isomerization to methylcyclopenta-structures, which are then in turn subject to ring opening to butyl side chains. These reactions only quantitatively depend on the structure of the molecule, and will be referred to as reaction families.

A QSRR within a reaction family is a link between molecular structure, as characterized by a reactivity index, and a rate, equilibrium, or adsorption constant. The literature [2,6,7,9,17] suggests that thermochemical quantities, such as enthalpies of formation of stable molecules and carbocation intermediates, may be appropriate reactivity indices for acid-catalyzed reactions. Semi-empirical molecular orbital calculations were thus used to make the structure-index link for the establishment of QSRRs. The calculation procedure was identical to that described elsewhere [9], and the standard enthalpies of formation were used (25°C, gaseous state). Carbocation intermediates were constructed by protonation of the stable molecule on the aromatic ring closest to the naphthenic ring subject to the acid center transformation. If more than one carboca-

Table 2
Standard enthalpies of formation of molecules and carbocation intermediates in naphthalene/phenanthrene hydrocracking sequence. Calculated with MOPAC v. 6.00. AM1 Hamiltonian was used. H_f = enthalpy of formation (kcal/mol); ΔH_r^0 = enthalpy of reaction (kcal/mol); $\Delta H_f^0(+)$ = enthalpy of formation of the carbocation intermediate (kcal/mol)

Reactant	H_f reac.	H_f inter.	H_f prod.	Product	ΔH_r^0	$\Delta H_f^0(+)$
Phenanthrene	57.47		20.16	tetrahydrophenanth.	−37.31	
Tetrahydrophenanth.	20.16	190.11	26.80	*i*-tetrahydrophenanth.	6.65	169.95
i-Tetrahydrophenanth.	26.80	197.47	16.56	*n*-butyl naphthalene	−10.25	170.67
Tetrahydrophenanth.	20.16		−19.82	*sym*-octahydrophen.	−39.97	
sym-Octahydrophen.	−19.82	154.57	−14.19	*i-sym*-octahydrophen.	5.63	174.38
i-sym-Octahydrophen.	−14.19	162.37	−23.20	5- and 6-butyl tetralins	−9.01	176.55
Tetrahydrophenanth.	20.16		−13.58	*asym*-octahydrophen.	−33.74	
asym-octahYdrophen.	−13.58	168.24	−5.39	*i-asym*-octahydroph.	8.19	181.82
i-asym-Octahydroph.	−5.39	175.53	−22.27	1- and 2-butyl tetralins	−16.88	180.92
Naphthalene	38.36		0.47	tetralin	−37.89	
Tetralin	0.47	182.65	4.27	1-methyl indan	3.81	182.18
1-Methyl indan	4.27	189.74	−4.08	*n*-butyl benzene	−8.35	185.47

tion structure was possible, the structure with the lowest enthalpy of formation (ΔH_c^+) was selected. Calculation results are summarized in Table 2.

The results of the molecular orbital calculations allow scrutiny of the trends in carbocation stability. The postulated intermediate carbocations of Table 2 are energetically demanding, and the value of the enthalpy of formation (ΔH_c^+) depends on the ability of the unit sheet to stabilize a positive charge. Thus the lowest enthalpies of formation (the most stable structures) are exhibited by the 2-aromatic ring structures in tetrahydrophenanthrene and *iso*-tetrahydrophenanthrene, and the highest in tetralin and 1-methylindan (Table 2). The inductive effect of the saturated ring in octahydrophenanthrenes further assists in stabilizing the carbocation, compared to tetralin. Therefore, ΔH_c^+ as a reactivity index describes quite well the observed trends in reactivity for both isomerizations and ring openings. The use of the standard enthalpy of reaction (ΔH_r^0) as a reactivity index for PNA hydrogenations was established elsewhere [14].

The existence of such correlations between rate parameters and energetic quantities (ΔH_c^+) can be traced to either strict adherence to the isoentropic reaction family concept and/or the existence of implicit, compensating, correlations between enthalpic (E^*) and entropic (ln A) quantities in the Arrhenius formalism [Eq. (2)]. Thus the development of temperature-independent QSRRs for each reaction family can be viewed, essentially, as a model of the variation of the activation energies (E^*) and pre-exponential factors (ln A) within a reaction family. The concept of a reaction family can thus exploit either a constant pre-exponential factor, or one that "compensates" with changes in activation energy. The latter approach, adding flexibility, was used to relate changes in pre-exponential factors within a family to changes in activation energies, and, by association, to ΔH_c^+.

This can also apply directly to reaction enthalpies and entropies in equilibrium parameters. The principle of compensation offers a

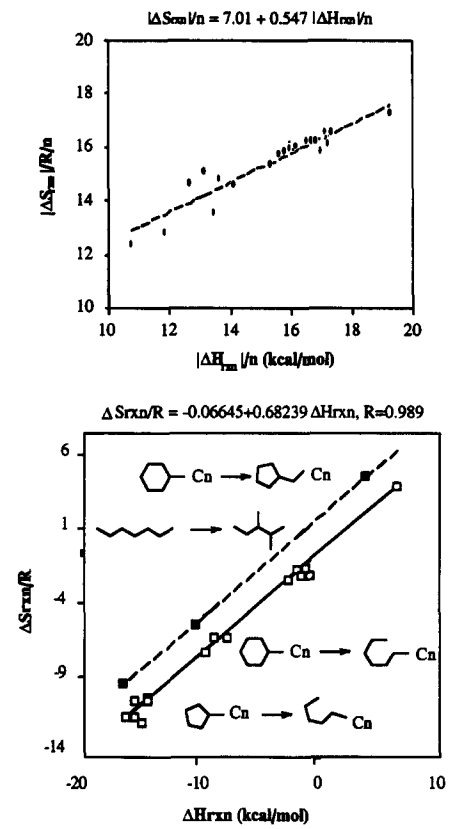

Fig. 4. Correlation between enthalpies and entropies of reaction (a) for polynuclear aromatic hydrogenation ([9], data from [18]) and (b) cyclohexane isomerizations and cyclohexane and methyl cyclopentane ring openings (data from [19]). (---) Constant reaction entropies; (————) continuous line represents correlation.

convenient simplification in enthalpies and entropies of hydrogenation of polynuclear aromatics (Fig. 4a, from [14], experimental data from [18]). Precedent for compensation in equilibrium constants for acid center transformations is developed in Fig. 4b, where the variation of reaction entropies with reaction enthalpies for isomerization reactions of *n*-hexane, *iso*-hexanes, and cyclohexanes, and ring opening reactions of cyclohexa- and methylcyclopenta-rings are presented (experimental data from [19]).

Linear regression on the data of Fig. 4b revealed that the "compensation-based" correlation was more appropriate than the "constant entropy" assumption, and resulted in a broader

correlation. The best-fit equation for reaction entropies encompassed both isomerization and ring opening reactions. This information suggests the usefulness of the compensation notions in the development of QSRRs for the isomerization and ring opening reactions during PNA hydrocracking. Moreover, it suggests that isomerization and ring opening reaction quantities can be described with the same equations.

4. Development of QSRRS

The reaction family concepts described above were used to set the functional form for temperature-independent structure/reactivity relationships for rate, equilibrium and adsorption constants, as follows.

4.1. Acid centers: isomerization and ring opening rate, equilibrium, and adsorption constants

The rate constants for the acid center transformations of isomerization and ring opening were described with ΔH_c^+ and temperature as the variables. The Arrhenius expression of Eq. (2) allows illustration,

$$\ln k = \ln A - E^*/RT \tag{2}$$

where ln A is the natural logarithm of the pre-exponential factor and E^* the apparent activation energy. The quantities ln A and E^* were assumed constant over the temperature interval of interest. The LFER approximation allows E^* to be linearly correlated to the reactivity index, ΔH_c^+ [Eq. (3)]:

$$E^* = c + d\Delta H_c^+ \tag{3}$$

and, exploiting the notion of a reaction family with compensation, ln A was in turn linearly correlated to E^* [Eq. (4)]:

$$\ln A = a + bE^* \tag{4}$$

This allowed the Arrhenius relation of Eq. (2) to be rewritten for isomerization in terms of the variables ΔH_c^+ and T and the parameters a, b, c, d, as Eq. (5):

Isomerization rate:

$$\ln k = a_i + c_i(b_i - 1/RT) + d_i(b_i - 1/RT) \times \Delta H_c^+ \tag{5}$$

For ring opening, Eq. (6) was modified to account for a hydrogen partial pressure dependence.

Ring opening rate:

$$\ln k = \ln P_{H_2} - a_R + c_R(b_R - 1/RT) + d_R(b_R - 1/RT)\Delta H_c^+ \tag{6}$$

The requirement for positive activation energies results in $(c + d\ \Delta H_c^+) > 0$ in the area $150 < \Delta H_c^+ < 250$. This results in the requirement $d > |c/250|$. For both isomerizations and ring openings (see Table 2), this gives $d = 0$ [1]. The requirement for the rate parameter, k, to decrease with increasing ΔH_c^+ results in $d(b - 1/RT) < 0$. Since $d > 0$, parameter b was bound by $b < 1/RT$. In the temperature interval of interest, this translates to $b < 0.78$. Linear regression of the rate constant data yielded initial guesses for the parameters a, b, c, d.

The concept of compensation was also used to evaluate QSRRs for equilibrium constants for acid center transformations. The appropriate indices for equilibrium constants are the enthalpy and entropy of reaction. Values of ΔH_r^0 for the reactions of interest were presented in Table 2. Values of ΔS_r^0 are less readily obtained. However, the occurrence of compensation provides a first-pass estimate. This can be summarized with the van't Hoff equation as the starting point:

$$\ln K_{eq} = \Delta S_r^0/R - \Delta H_r^0/RT \tag{7}$$

To the extent that the reaction entropy changes could be linearly correlated with reaction enthalpy changes, as in Eq. (8):

$$\Delta S_r^0/R = A + B\Delta H_r^0 \tag{8}$$

the van't Hoff equation Eq. (7) can be rewritten in terms of the variables ΔH_r^0 and temperature, as in Eq. (9):

Isomerization/ring opening equilibrium:

$$\ln K_{eq} = A + (B - 1/RT)\Delta H_r^0 \tag{9}$$

The adsorption constants on the acid sites were correlated according to Eq. (10), as described elsewhere [9]. Its variables are the number of aromatic rings (N_{AR}) and the number of saturated carbons (N_{SC}).

Acid center adsorption:

$$\ln K_{ads} = Z_1 + (Z_2 N_{AR} + Z_3 N_{SC})/RT. \quad (10)$$

4.2. Metal centers: hydrogenation rate, equilibrium and adsorption constants

The rate, equilibrium, and adsorption constant correlations [Eqs. (11)–(14)] for reactions on the metal sites were developed elsewhere [9]. The temperature dependence of adsorption constants was that of Eq. (14). In Eqs. (11)–(14), the variables are the MOPAC/AM1 calculated standard enthalpy of reaction (ΔH_r^0), hydrogen stoichiometry (n), the number of aromatic rings (N_{AR}) and the number of saturated carbons (N_{SC}). Hydrogen pressure (P_{H_2}) and temperature (T) were explicitly accounted for.

Hydrogenation rate:

$$\ln k = \ln K_{ads} + n \ln P_{H_2} + \ln A_H - E_H^*/RT; \quad (11)$$

$$\ln A_H = -(A_{1H} + A_{2H} n); \; E_H^* = A_{3H}|\Delta H_r^0|. \quad (12)$$

Hydrogenation equilibrium:

$$\ln K = -B_H n + (1/RT - 0.54707)|\Delta H_r^0|. \quad (13)$$

Metal center adsorption:

$$\ln K_{ads} = M_1 + (M_2 N_{AR} + M_3 N_{SC})/RT. \quad (14)$$

In summary, for acid center transformations, the forward rate constants for the four isomerizations were estimated using four parameters, a_i, b_i, c_i, and d_i; another four parameters, a_R, b_R, c_R, and d_R, were used to estimate the forward rate constants for the five ring opening reactions, and the corresponding nine equilibrium constants were estimated using two parameters, A and B. The 17 adsorption constants on the acid sites for each of the eight temperatures were estimated using three parameters, Z_1, Z_2, and Z_3; A total of 280 constants (72 rate, 72 equilibrium, and 136 adsorption) needed to describe isomerization and ring opening kinetics in the temperature interval 300–370°C were reduced to 13 temperature-independent parameters.

Similarly, for metal center transformations, the forward rate constants needed for the 10 hydrogenation reactions of the network in Fig. 3 were estimated using three parameters, A_{1H}, A_{2H}, and A_{3H}, and the corresponding 10 equilibrium constants were estimated using one parameter, B_H. The 17 adsorption constants on the metal sites for each of the eight temperatures were estimated using three parameters, M_1, M_2, and M_3. A total of 296 constants (80 rate, 80 equilibrium, and 136 adsorption) needed to describe hydrogenation kinetics in the temperature interval 300–370°C were reduced to these seven temperature-independent parameters.

5. Parameter estimation results

The parameter estimation was performed directly to the concentration vs. time experimental data from naphthalene/phenanthrene hydrocracking in the temperature interval 300–370°C. This represented regression to approximately 1800 experimental concentrations. The correlations of Eqs. (5)–(10) were imposed for the relevant reaction family to summarize a total of 304 rate and equilibrium constants, and the 34 adsorption constants on the metal and acid sites. Constraints for the QSRR parameters were described above. Parameter estimation was also constrained for non-negative rate, equilibrium, and adsorption constants in the reactivity index interval of interest.

The parameter estimation results showed that the values of the slopes of Eq. (3) and Eq. (4) were inversely correlated for both isomerization and ring openings, i.e. $d_i = 1/b_i$; $d_R = 1/b_R$. In addition, the values for the slopes of Eq. (5)

and Eq. (6) were statistically identical for isomerizations and ring openings, i.e. $b_i = b_R$. When these constraints were added, the number of parameters was further reduced from 20 to 17.

The final QSRR correlations summarize the results. These are given in Eqs. (15)–(24):

5.1. Hydrogenations

Adsorption:

$$\ln K_{ads} = 1.324 + (0.887N_{AR} + 0.123N_{SC})/RT \quad (15)$$

Equilibrium:

$$\ln K = -7.017n + (1/RT - 0.54707)|\Delta H_r^0| \quad (16)$$

Rate:

$$\ln k = \ln K_{ads} + n \ln P_{H_2} + \ln A_H - E_H^*/RT \quad (17)$$

$$\ln A_H = -(6.613 + 5.767n); \quad E_H^* = 0.228|\Delta H_r^0| \quad (18)$$

5.2. Acid center transformations

Adsorption:

$$\ln K_{ads} = 0.182 + (1.934N_{AR} + 0.187N_{SC})/RT \quad (19)$$

Equilibrium:

$$\ln K = -1.775 + (1.469 - 1/RT)\Delta H_r^0 \quad (20)$$

Isomerizationrate:

$$\ln k = -2.89 - 305(0.585 - 1/RT) + (1 - 1/0.585RT)\Delta H_c^+ \quad (21)$$

$$(E_i^* = -305 + 1.709\Delta H_c^+; \quad \ln A_i = -2.89 + 0.585E_i^*) \quad (22)$$

Ringopeningrate:

$$\ln k = \ln P_{H_2} - 4.64 - 271(0.585 - 1/RT) + (1 - 1/0.585RT)\Delta H_c^+(6) \quad (23)$$

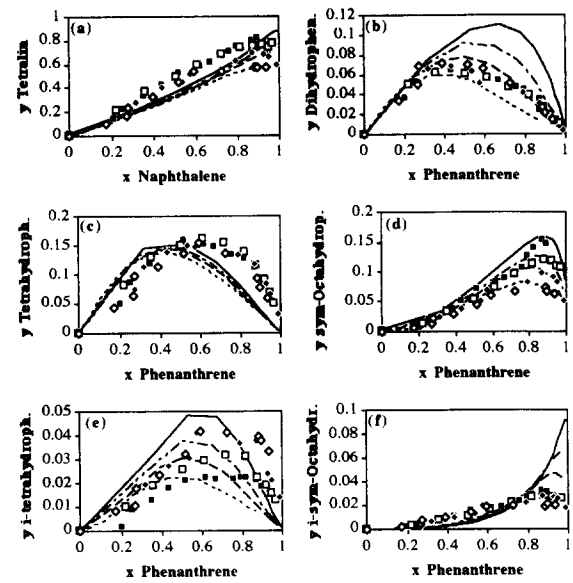

Fig. 5. Comparison between experimental and QSRR-calculated yields of phenanthrene and naphthalene hydrocracking products. (a) Tetralin; (b) dihydrophenanthrene; (c) tetrahydrophenanthrene; (d) *sym*-octahydrophenanthrene; (e) *i*-tetrahydrophenanthrene; (f) *i-sym*-octahydrophenanthrene. Lines represent results with the QSRR best-fit parameters of 15161718192021222324. (■) 300°C; (□) 320°C; (♦) 340°C; (◇) 365°C.

$$(E_{RO}^* = -271 + 1.709\Delta H_c^+; \quad \ln A_{RO} = -4.64 + 0.585E_{RO}^*) \quad (24)$$

Fig. 5 summarizes these parameter estimation results in terms of a set of yield vs. conversion plots for key products. The predictions follow the experimental data quite closely, considering the reduction in the number of parameters from Fig. 3 (576) to Fig. 5 (17).

6. Discussion

The best-fit values for the correlations in Eqs. (15)–(23) give additional insight into the temperature dependence of hydrogenation and hydrocracking reactions. The enthalpy of adsorption on the metal sites, as calculated from Eq. (15), was a function of both the number of aromatic rings and the number of saturated carbons. The enthalpy of adsorption increased with

both indices, and was lower than 3 kcal/mol. This is also true of the enthalpy of adsorption on the acid sites [Eq. (19)]. The highest value was that for phenanthrene (5.8 kcal/gmol).

The activation energies for hydrogenations were correlated with the reaction enthalpy [Eq. (18)]; as a result, their values were highest for benzenic and lowest for phenanthrenic hydrogenations. The pre-exponential factors [Eq. (18)] also had a best fit hydrogen number dependence characterized by the coefficient of 5.767. Note that the single optimized parameter in the QSRR for hydrogenation equilibrium constants [Eq. (16)] was very close to the value reported earlier [9]. (7.017 vs. 7.014).

Eqs. (21)–(24) for isomerization and ring opening reactions showed that activation energies were a sensitive function of ΔH_c^+, as a coefficient of 1.709 was obtained. For both reaction families, the pre-exponential factors were a relatively weak function of the activation energies (coefficient 0.585). Eq. (20) for isomerization and ring opening equilibrium constants showed that the reaction entropies varied significantly with reaction enthalpies (coefficient 1.469).

Clearly, for both reaction and activation, the entropic quantities varied from one member of the reaction family to another and thus diverged from the strict Hammett notions of the same reaction entropy for each member of the reaction family. However, the compensation constraint between enthalpic and entropic quantities evidently provided a reasonable approximation of the chemistry. The flexibility provided by the compensation scenario allowed for the development of simple but useful correlations.

The functional form of the QSRRs presented in this paper is general enough to be independent of the specific catalyst, and it may be used to correlate kinetic parameters for other bifunctional hydrocracking catalysts. In this case, however, the quantitative values of the QSRR parameters must be optimized with respect to hydrocracking data over the catalyst under consideration.

7. Summary

Phenanthrene/naphthalene mixture hydrocracking at different temperatures offered information on Arrhenius and van't Hoff parameters for the metal and acid center transformations in the reaction network. Fitting the Arrhenius and van't Hoff expressions for rate, equilibrium, and adsorption parameters provided quantitative rate laws. Activation energies for hydrogenations were low, but in agreement with the values reported in the literature. Activation energies for acid center transformations were significantly higher, of the order of previously reported values. In both isomerizations and ring openings, pre-exponential factors varied proportionally to the activation energies with quite acceptable precision.

The number of parameters needed to describe hydrocracking kinetics was reduced by the development of temperature-independent quantitative structure/reactivity correlations for the activation energies and entropies and the reaction and adsorption entropies. This approach can be summarized in the quantitative structure/reactivity relationships of Eqs. (15)–(24) for the calculation of rate, equilibrium, and adsorption constants. In turn, this allowed the kinetics of naphthalene and phenanthrene hydrocracking to be represented very satisfactorily, over a wide temperature range in terms of just 17 quantitative structure/reactivity correlations parameters. These 17 parameters summarized the chemical information in 576 rate, equilibrium, and adsorption constants, which shows that the QSRR approach reduced the number of modeling parameters by about 97%.

References

[1] L.P. Hammett, Physical organic chemistry, McGraw-Hill, New York, 1940.
[2] I. Mochida and Y. Yoneda, J. Catal., 7 (1967) 386–392.
[3] I. Mochida and Y. Yoneda, J. Catal., 7 (1967) 393–396.
[4] H. Matsumoto, J.-I. Take and Y. Yoneda, J. Catal., 12 (1968) 211–219.

[5] I.J. Dunn, J. Catal., 12 (1968) 335–340.
[6] R.N. Landau, S.C. Korre, M. Neurock, M.T. Klein and R.J. Quann, in Catalytic hydroprocessing of petroleum and distillates, Marcel Dekker, 1994, pp. 421–432
[7] M. Neurock and M.T. Klein, Polyc. Arom. Compounds, 3 (1993) 231–246.
[8] M.T. Neurock, A computational chemical reaction engineering analysis of complex heavy hydrocarbon reaction systems, Ph.D. Thesis, University of Delaware, 1992.
[9] S.C. Korre, M. Neurock, M.T. Klein and R.J. Quann, Chem. Eng. Sci., 49 (1995) 4191–4210.
[10] I. Mochida and Y. Yoneda, J. Catal., 8 (1967) 223–230.
[11] S.A. Qader and G.R. Hills, Am. Chem. Soc., Div. Fuel Chem. Prepr., 16 (1972) 93–106.
[12] P. Kokayeff, AIChE Spring Annual Meeting and Petrochemical Exp., Houston, TX, 1993.
[13] S.C. Korre, M.T. Klein and R.J. Quann, Ind. Eng. Chem. Res., submitted.
[14] S.C. Korre, M.T. Klein and R.J. Quann, Ind. Eng. Chem. Res., 34 (1995) 101–117
[15] S.C. Korre, Quantitative structure/reactivity correlations as a reaction engineering tool: application to hydrocracking of polynuclear aromatics, Ph.D. Dissertation, University of Delaware, 1995.
[16] G.F. Froment and K.B. Bischoff, Chemical reactor analysis and design, Wiley, New York, 1990.
[17] H. Machácek, K. Kochloefl and M. Kraus, Collect. Czech. Chem. Commun., 31 (1966) 576–584.
[18] C.G. Frye, J. Chem. Eng. Data, 7(4) (1962) 592–595.
[19] R.H. Perry and D.W. Green (Eds.), Perry's chemical engineers' handbook, McGraw-Hill Chem. Eng. Ser., McGraw-Hill, New York, 1984.